ELSEVIER

Contents lists available at ScienceDirect

International Journal of Biological Macromolecules

journal homepage: www.elsevier.com/locate/ijbiomac



Identification of i-motifs in Alphaherpesvirus immediate early promoters and their dynamic folding with G4s during infection

Emanuela Ruggiero ^a, Filippo Mattellone ^a, Daniel Christ ^b, Sara N. Richter ^{a,c,*}, Ilaria Frasson ^{a,**}

- ^a Department of Molecular Medicine, University of Padova, 35121 Padova, Italy
- ^b Garvan Institute of Medical Research, Immunology Department, 384 Victoria Street, Darlinghurst, Sydney, NSW, 2010, Australia
- ^c Microbiology and Virology Unit, Padova University Hospital, 35121 Padova, Italy

ARTICLE INFO

Keywords: i-motif G-quadruplex Viral transcription Alphaherpesviruses

ABSTRACT

I-motifs (iMs) and G-quadruplexes (G4s) are non-canonical DNA secondary structures formed by C-rich and G-rich sequences, respectively. While G4s have been identified as regulatory elements in both human and viral genomes, iMs remain largely unexplored. This study investigates the presence of iMs in the immediate-early (IE) promoters of human Alphaherpesviruses (αHHVs), namely herpes simplex virus 1 (HSV-1), herpes simplex virus 2 and varicella-zoster virus. αHHVs IE promoters, crucial for initiating an efficient viral cycle, embed G4s, but the potential presence of iMs in these regions is unknown.

We identified highly conserved putative iM-forming sequences in IE promoters of all α HHVs. Biophysical characterization by circular dichroism, thermal difference spectroscopy and bromine footprinting, confirmed the ability of these sequences to form iMs in vitro, with varying conformations and distributions among the three viruses

Using a CUT&Tag-qPCR assay, we detected and quantified both iM and G4 structures in the HSV-1 genome during active viral infection. Our results show the dynamic formation of iMs and G4s in IE promoters, with enrichment levels changing over time. These structural changes correlated with variations in IE gene expression, indicating a functional role in HSV-1 biology.

This study provides the first evidence of iMs in a viral genome, revealing a novel layer of genome organization through iMs folding alongside G4s in viruses.

1. Introduction

Herpes simplex virus 1 (HSV-1) is a common infectious agent spread by skin-to-skin contact, affecting almost 4 billion people worldwide [1]. It commonly causes vesicular lesions but can also lead to severe complications such as encephalitis and keratitis [2]. Upon infecting the human cells, the viral genome enters the host cell nucleus where the viral genes are transcribed in a coordinated cascade, starting from the five immediate-early (IE) genes, which include ICPO, ICP4, ICP22, ICP27 and ICP47 [3–7]. The mechanisms governing IE gene expression regulation, from initial inhibition to varied expression levels, remain incompletely understood. While human and viral transcription factors are known to recognize specific nucleotide sequences, recent studies

suggest they may also recognize DNA secondary structures [8–10]. This regulatory model, studied in HSV-1, likely extends to the other human Alphaherpesviruses (α HHVs), Herpes Simplex Virus-2 (HSV-2) and Varicella Zoster Virus (VZV), with variations potentially explaining their distinct biological behaviours and host cell tropisms.

Non-canonical DNA structures, such as i-motifs (iMs) and G-quadruplexes (G4s), have garnered interest for their regulatory roles in gene expression at the human level and recently in microorganisms [11,12]. G4s form in guanine (G)-rich genomic regions through the formation of stacked G-quartets [13]. The presence of G4s has been reported in many important human viral pathogens [14], including Retroviruses [15–18], Arboviruses [19,20] and α HHVs [21–23].

In this context, we previously identified highly conserved G4-

^{*} Correspondence to: Sara N. Richter, Department of Molecular Medicine, University of Padova and Microbiology and Virology Unit, Padova University Hospital, 35121 Padova, Italy.

^{**} Correspondence to: Ilaria Frasson, Department of Molecular Medicine, University of Padova, 35121 Padova, Italy. E-mail addresses: sara.richter@unipd.it (S.N. Richter), ilaria.frasson@unipd.it (I. Frasson).

forming sequences in HSV-1 IE promoters, able to fold into multiple parallel and stable G4s, with ICPO, ICP4, ICP22, and ICP47 promoters showing the highest numbers. Interestingly, despite their different genomic locations, ICP22 and ICP47 promoters share identical sequences and G4-forming patterns [21,24]. In addition, ICP4, the main transcription factor of HSV-1, was shown to bind and unfold G4s, including those in its promoter, and promote transcription [10]. G4 stabilization by the ligand BRACO-19 downregulated promoter activity, suggesting these structures might play a role in viral transcriptional regulation. G4-forming sequences were also found in IE gene promoters of the other human $\alpha HHVs$ [21]. The genomic segments complementary to G4s are cytosine (C)-rich and so prone to form iMs, which are intercalated structures arising from hemiprotonated C-C⁺ H-bonds [25]. The development of the iM-specific antibody iMab [26-28] expanded iM investigation in humans, revealing that iMs may function as regulatory switches influencing gene expression through their folding and stabilization dynamics [25,26,29-31]. In viral genomes, the presence and function of iMs remain largely unexplored, with just one in vitro investigation regarding the long terminal repeat promoter of the human immunodeficiency virus type 1 proviral genome, where a unique iM structure with a central stem-loop was recognized by the hnRNPK cellular protein and modulated transcription [32]. Nonetheless, studies on iMs within viral promoters, such as those of αHHVs, are lacking. Understanding whether iMs fold within these viral regulatory regions during infection is essential for elucidating their role in viral gene expression and replication. To address this gap, we integrated biophysical characterization and a CUT&Tag-qPCR assay to investigate the presence and folding dynamics of iMs in the IE promoters of αHHVs. Our study aimed to identify putative iM-forming sequences (PiMSs) within αHHVs IE promoters, assess their folding capabilities in vitro, and monitor their formation during viral infection in human cells alongside G4s (Fig. 1).

2. Methods

2.1. Viral genomes selection, G4 and iM prediction, and conservation analysis

The complete set of human α HHVs genome sequences was downloaded from the GenBank database at NCBI, including the HSV-1 reference genome NC_001806.2, HSV-2 NC_001798.2 and VZV NC_001348.1. In the case of HSV-1 and HSV-2, regions up to 1 kilobase upstream of the transcription start sites of the five IE genes (ICP0, ICP4, ICP27, ICP22, ICP47) were analysed for promoter-associated features, such as TATA boxes and replication origins. This analysis was conducted to improve the characterization of the promoter regions. The promoter regions were scanned for potential G4 forming sequences (PQSs) with the following criteria $[G(2)L(1-7)]_4$, $[G(3)L(1-12)]_4$ and $[G(4)L(1-12)]_4$, utilizing the QGRS and Quadbase2 prediction programs on

both strands [33,34]. The identified PQSs were manually curated for non-canonical G4s, such as those with a loop of zero nucleotides and/or bulged G-tracts. A comprehensive search of literature was conducted for homologous genes of the HSV-1 virus in the context of VZV. Subsequently, these genes were subjected to promoter analysis, utilizing identical parameters to ensure a uniform and rigorous approach [21]. The C-rich regions were calculated as reverse complemented sequences. In both ICP4 and ICP22/ICP47 promoters, we had previously identified PQSs containing more than four G-stretches, including one tract that could participate to G4 folding upon the inclusion of a bulge. In these cases, the regions were subdivided into adjacent and partially overlapping G4s for analysis. To ensure consistency, we applied the same division in our iM analysis.

For conservation analyses, viral sequences retrieved from the NCBI genome database (as of December 2024) were subjected to a filtration process, whereby unverified or partially sequenced genomes, as well as genome sequences containing multiple stretches of nucleotides lacking base assignments (i.e. NNN), were removed. The genomes were aligned using the SnapGene (https://www.snapgene.com/) software, and the conservation of retrieved PiMSs was analysed using WebLogo [35].

2.2. Circular dichroism (CD)

Oligonucleotides (Table 1) were prepared to 2 μ M final concentration in 20 mM phosphate buffer, 80 mM KCl, over a pH range of 5.4–7.4. Samples were denatured at 95 °C for 5 min and then slowly cooled to room temperature (RT) overnight. CD spectra were recorded on a Chirascan-Plus equipped with a Peltier temperature controller using a quartz cell with a 5 mm optical-path length. CD spectra were measured at 20 °C from wavelength 230 to 320 nm and baseline-corrected for buffer contribution. The obtained ellipticities were converted to mean residue ellipticity expressed in deg \times cm² \times dmol⁻¹ (molar ellipticity). CD spectra were plotted using RStudio software (RStudio 2023.12.0) for windows. Posit team (2025). RStudio: Integrated Development Environment for R. Posit Software, PBC, Boston, MA. URL http://www.posit.co/.

2.3. Thermal difference spectra (TDS)

Samples were prepared diluting oligonucleotides to 2 μM final concentration in 20 mM phosphate buffer, 80 mM KCl over a pH range of 5.4–7.4. Samples were heated at 95 °C for 5 min and then slowly cooled to RT overnight. Absorption spectra were recorded on Perkin Elmer Lambda 25 UV/VIS Spectrophotometer equipped with Peltier temperature control system. Spectra were acquired in the range of 220 nm to 330 nm, with a scan speed of 120 nm/min. Measurements were taken at 90 °C and 15 °C, representing the unfolded and folded states, respectively. Spectra were obtained by subtracting the absorption spectra at 15 °C from those at 90 °C using UV WinLab Data Processor & Viewer

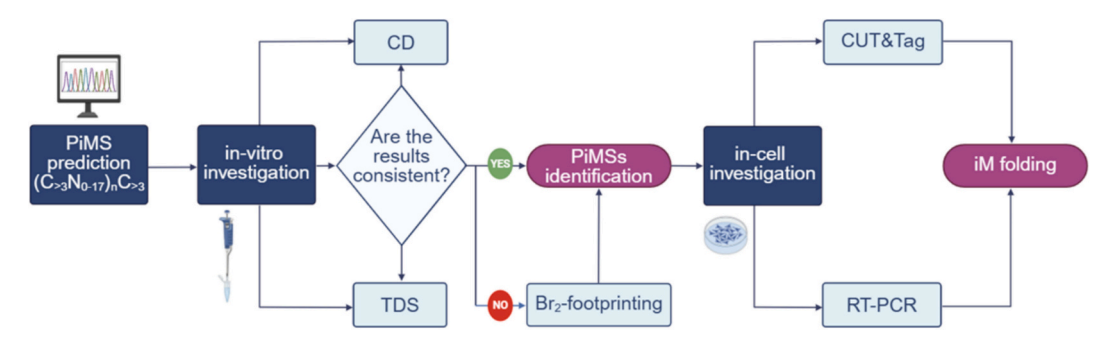


Fig. 1. Workflow for the identification and characterization of putative iM-forming sequences (PiMSs) in α HHVs IE genes. The process begins with sequences previously identified by bioinformatic analysis, followed by in vitro investigation using Circular Dichroism (CD) and Thermal Difference Spectra (TDS) techniques. If results are consistent, PiMSs are defined; if not, bromine footprinting is employed for further validation. PiMSs undergo in-cell investigation using CUT&Tag and RT-PCR to assess viral iM folding dynamics in the cellular environment.

software. Final plots were obtained with RStudio software.

2.4. Bromine footprinting

The bromine footprinting assay was performed as previously reported [32]. 5'-radiolabelled oligonucleotides were resuspended in 20 mM phosphate buffer at the indicated pH and 80 mM KCl, heat-denatured, and cooled overnight. 5 pmol/sample were incubated with in-situ generated molecular bromine by adding KBr and KHSO₅. The reaction was terminated with 0.3 M sodium acetate and calf thymus DNA solution, while unreacted bromine was removed by ethanol and tRNA precipitation. Subsequently, the DNA pellet was dried, resuspended in a 10 % piperidine solution in water and incubated at 90 °C for 30 min. Samples were dried, washed, and resuspended in sequencing gel loading dye before visualization on a 20 % denaturing PAGE with 7 M urea. Marker reactions were performed using formic acid for purine-specific cleavage [36]. Gels were visualized by phosphorimaging (Typhoon FLA 9000, GE Healthcare Europe) and quantified using ImageQuant TL Software (GE Healthcare Europe).

2.5. Cell line, virus and infection

Human bone osteosarcoma cells (U-2 OS, European Collection of Authenticated Cell Cultures (ECACC), #92022711) were cultured in Dulbecco's Modified Eagle Medium (DMEM, Gibco, LifeTechnologies, #41965062) supplemented with 10 % Fetal Bovine Serum (FBS, Gibco, LifeTechnologies, #10270106) and $1 \times$ Penicillin–Streptomycin (Gibco, LifeTechnologies, #15140122). HSV-1 strain 17+ (National Collection of Pathogenic Viruses, 0104151v) was propagated on U-2 OS cells.

U-2 OS cells (2.2×10^5 /well) were seeded in 6-well plates and infected for 1 h at a multiplicity of infection (MOI) of 2 plaque-forming units (PFU) per cell. Cells were harvested at 1- and 4-hours post-infection (hpi) for both CUT&Tag and expression analyses.

2.6. CUT&Tag-qPCR

The CUT&Tag protocol was performed as previously described [31]. Three independent biological replicates for each condition were performed. For each condition tested, 3×10^5 U-2 OS cells were harvested, washed with wash buffer and then immobilized on previously activated Concanavalin A-coated magnetic beads (conA-beads, Bangs Laboratories) for 20 min at RT on an end-over-end rotator. ConA-beads (10 ml/ sample) were activated in binding buffer and bead-bound cells were incubated with 50 µl of antibody binding buffer overnight at 4 °C with the following primary antibodies: anti-mouse IgG (1:100, Merck Millipore, #06-371), FLAG-tagged BG4 (500 ng), and FLAG-tagged iMab (4 μg, Absolute antibody, #Ab01462-30.135). Recombinant FLAG-tagged BG4 antibody was produced as previously reported [37]. BG4- and iMab-incubated cells were resuspended in 100 µl of antibody buffer with the mouse anti-FLAG antibody (anti-FLAG M2, 1:100, Sigma Aldrich, #F3165) for 1 h at RT. The secondary antibody binding was performed in 100 μ l of dig-wash buffer for 1 h at RT using: anti-mouse IgG (1:100, Merck Millipore, #06-371) for the FLAG-tagged BG4 and iMab samples and anti-rabbit IgG (1:100, Rockland, #611-201-122) for anti-mouse IgG samples. Then, beads-bound cells were resuspended in 50 μl dig-300 buffer with 1:20 dilution of pA-Tn5 adapter complex (CUTANA $^{\text{TM}}$ pAG-Tn5 for CUT&Tag, EpiCypher, #15-1017) and nutated for 1 h at RT. Beads were washed with 800 µl dig-300 buffer, followed by tagmentation in 200 μl of tagmentation buffer for 1 h at 37 °C. Reactions were stopped by adding stop buffer and incubating for 1 h at 63 $^{\circ}\text{C}.$ DNA fragments present in the supernatants were recovered by phenolchloroform extraction using phase-lock tubes (Qiagen, #129046) and resuspended in 1 mM Tris-HCl pH 8 and 0.1 mM EDTA. DNA libraries were amplified with NEBNext HiFi 2× PCR Master mix (New England Biolabs, #M0541S) with uniquely barcoded i5 and i7 primers [38], using the following cycling conditions: 72 °C for 5 min; 98 °C for 30 s;

14 cycles of 98 °C for 10 s and 63 °C for 30 s; 72 °C for 1 min. Post-PCR clean-up was performed using Agencourt AMPure magnetic XP beads (Beckman Coulter, #A63881), with three incubations of $1.2\times$, $0.6\times$, and $1.2\times$ volume of beads, respectively. Libraries were eluted in 10 mM Tris-HCl pH 8 and quantified with dsDNA high-sensitivity kit for Qubit (InvitrogenTM QubitTM 3 Fluorometer, ThermoFisher Scientific). The immunoprecipitated samples were used to quantify G4 and iM enrichment via qPCR, using Fast SYBR PCR mix (Applied Biosystems) with the primers reported in Table S1.

2.7. RT-qPCR

U-2 OS cells were infected at MOI 2 and harvested at 1 and 4 hpi. Total RNA was extracted using the Total RNA Purification Kit (NorgenBiotek, Cat #48400) and quantified via Nanodrop 2000 (Thermo Scientific). RT-qPCR was performed using a QuantStudio7Pro (Applied Biosystems, Thermoscientific) with KAPA SYBR® FAST One-Step (Merck Life Science, Cat #SF1UKB). Each reaction contained 60 ng RNA and 200 nM of each primer. Thermal cycling conditions: 42 °C for 10 min, 95 °C for 3 min, followed by 40 cycles of 95 °C for 15 s and 60 °C for 30 s and followed by a melting curve cycle of 95° for 15 s, 60° for 1 min and 95 °C for 1 s. Negative controls were included in each PCR run. Experiments were performed in technical duplicate with two biological replicates. Data analysis was conducted using the $2^{-\Delta\Delta CT}$ method [39]. Primers are listed in Table S1.

3. Results

3.1. aHHVs IE promoters embed highly conserved putative iM-forming sequences

Following our previous characterization of G4 presence and folding in the α HHVs IE promoter regions, we investigated the presence of PiMSs in the complementary strand of the same genomic locations [21]. In detail, we explored 21 sequences in HSV-1, 12 sequences in HSV-2 and 6 sequences in VZV, corresponding to the regions previously reported for G4s (Table 1). The analysis considered PiMSs with canonical features, specifically C-tracts containing at least three C residues and loops ranging from zero to seventeen nucleotides in length. The abundance of PiMSs in α HHVs exhibits a positive correlation with gene promoter lengths, with the longest promoters harbouring the highest number of PiMSs (Table 1).

Further analysis revealed distinctive characteristics of αHHVs PiMSs, in terms of C-tracts length and number, as well as loops length and composition, suggesting complex iM folding patterns for each virus (Fig. 2). The number of C residues in each C-tract varied from three to nine Cs, while the number of C-tracts ranged from two to six. Loop lengths spanned from very short (1 nucleotide, e.g., HSV-1 ICP4 146666-C) to longer segments (up to 17 nucleotides, e.g., VZV ORF62/ORF63 109246-C), with some PiMSs alternating short and long loops. Loop composition analysis revealed further variability: A/T-rich loops, which might contribute to the flexibility of the structure, were observed, as well as G-containing loops, which could potentially participate in additional base-pairing interactions. Moreover, mixed composition loops comprising various combinations of A, T, and G residues were also identified. Alternating loop and C-tract lengths were also present, potentially resulting in asymmetric iM structures (e.g., HSV-1 ICP4 146678-C). We also considered PiMSs that might fold into iMs through incorporation of a bulge (e.g., HSV-1 ICPO 2009-C and HSV-2 ICPO 2066-C) (Table 1). Overall, HSV-1 PiMSs showed the highest variety in nucleotide loop composition, while no noticeable differences were observed in terms of lengths (Fig. 2).

To assess PiMS relevance in viral genomes, we analysed base conservation in each sequence across available viral fully sequenced isolates for HSV-1, HSV-2, and VZV (61, 15 and 157 aligned genomes, respectively). In all three viruses, most PiMSs exhibited the highest

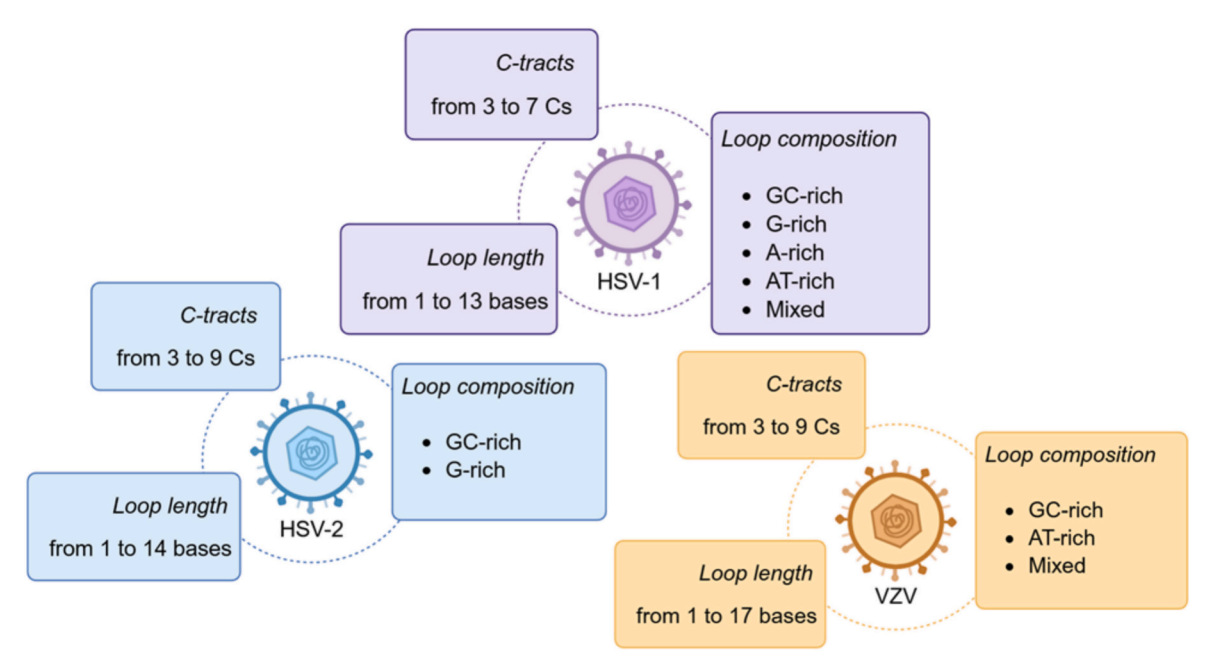


Fig. 2. Schematic representation of the PiMS analysis for each virus (HSV-1 in purple, HSV-2 in blue, VZV in orange). The figure illustrates the main features of PiMSs in each viral genome, including cytosine-tract (C-tract) length, loop length, and nucleotide composition of loops.

conservation, both in terms of C residues and loop sequences (Fig. 3), underscoring the potential critical importance of these sequences and iM structures in HHV biology. Notably, PiMSs located within extremely GC-rich viral repeat regions demonstrated poor alignment, which likely derives by the difficulty in sequencing and assembling highly G-rich DNA regions (e.g., HSV-1 ICP22/ICP47 132411 and 132424).

3.2. Comprehensive biophysics characterization of Alpha-HHV IE iM structures

To experimentally validate PiMS structural properties we determined their folding in vitro, employing two complementary biophysical techniques: Circular Dichroism (CD) and Thermal Difference Spectroscopy (TDS) [29,40,41]. The use of multiple spectroscopic methods is essential for accurate iM characterization, as it provides a comprehensive assessment of their folding and stability under various conditions [29,42]. Here, we systematically examined each PiMS under a range of pH conditions from 5.4 to 7.4, since pH is a critical factor for iM formation [29,43]. The iM structure is characterized in the CD spectrum by a positive peak at around 288 nm and a negative peak at 260 nm [44], while in the TDS profile by a positive peak at around 240 nm and a negative peak at 295 nm [41]. By comparing the CD and TDS profiles, we confirmed iM formation and assessed their pH-dependence (Table 1, Fig. 4 and S1). PiMSs were categorized into three groups: sequences demonstrating clear iM formation, therefore displaying all characteristic peaks at pH 5.4, were designated as positive (iM) (i.e. HSV-1 ICP4 R146532-C), whereas those exhibiting no evidence of iM folding were classified as 'no-iM' (i.e. HSV-1 ICPO 2009-C). Additionally, we introduced the 'iM-like' category to denote sequences displaying CD spectrum and/or TDS profile at acidic pH lacking one of the iM distinctive peaks, suggesting potential dynamic folding [45]. An example of this is HSV-1 ICP4 146666-C, which lacks a sharp minimum peak at 260 nm in the CD spectrum (Table 1).

In HSV-1, nine sequences (43 %) folded into iMs, yielding positive results in both CD and TDS analyses (Fig. 4 and S1). Eight sequences displayed inconsistent classifications between the techniques: this discrepancy suggests the formation of intermediate or low stability iM structures. One sequence was consistently categorized as iM-like by both techniques, indicating the presence of multiple conformations in

solution, including, but not limited to iMs (ICPO 1966-C). These may represent intermediate structures or non-canonical iMs and require further investigation to elucidate their structural properties. Three sequences were concordantly classified as no-iM structures by both techniques (ICPO 2009-C; ICP4 146947-C and ICP27 113501-C).

The analysis of PiMSs embedded in HSV-2 IE promoters revealed that five sequences (42 %) folded into iMs (Fig. 4 and S1). Seven sequences exhibited subtle differences in structural characterization between the two techniques, with TDS indicating clear iM formation and CD spectroscopy suggesting iM-like properties. This highlights a nuanced scenario regarding iM formation in the HSV-2 IE promoter regions, where more than half of the sequences were classified as iM-like by CD but categorized as definitive iMs by TDS (Table 1).

In VZV promoter regions, only one sequence (17 %) demonstrated distinct iM folding (ORF61 105081-C) (Fig. S1). One sequence consistently displayed iM-like characteristics in both spectroscopic techniques (ORF61 109703-C). Three PiMS were classified as iM-like by CD analysis, yet TDS categorized it as iM structures (ORF61 R104021-C, ORF62/ORF63 109246-C and R110410-C). The remaining sequence showed noiM formation potential in either technique (ORF4 4278-C) (Table 1).

For all confirmed iM- and iM-like-forming sequences the transitional pH (pH $_{\rm T}$) was calculated (Table S2) whenever feasible, with values ranging from 5.6 to 6.9.

To better elucidate the structural characteristics of sequences that displayed inconsistent classifications between CD and TDS analyses and were categorized as iM-like structures, we performed bromine footprinting analysis (Figs. 5, S2). This method exploits the preferential reactivity of bromine with unpaired cytosines, allowing for the identification of accessible nucleotides, thus the C residues not involved in iM formation. We tested each iM-like structure at pH 5.4, 6 and 7.4, so to define pH-dependent iM formation. Sequences classified as positive (HSV-1 ICP4 R146532-C) or negative iMs (HSV-1 ICP0 2009-C) in both CD and TDS analyses served as controls (Fig. S2). Comparing the protection pattern at the three tested pH values, two sequences showed clear iM configurations, with four intercalated C-tracts involved in iM formation (HSV-1 ICP4 146666-C, VZV ORF61 R104021-C). Conversely, the presence of mixed conformations in solution was confirmed for six sequences, suggesting a dynamic equilibrium between iM, and additional alternative structures and unstructured conformations. One

Promoter	Name	WEBLOGO	Promoter	Name	WEBLOGO	
	HSV-1	(61 genomes)	HSV-2 (15 genomes)			
ICP0	1875-C	*CCCCAAAGAACCCCATTAGCATGCCCCTCCCGC		R1571-C	I_COORGE CTCCCCCCCCCCCCCCCCCCCCCCCCCCCCCCCCCCC	
	1881-C	* CCCCGGTGTCCCCCCAAACAACCCCATTACCATCCCCC	ICP0	1913-C	ECCONTRACTOR CONTRACTOR FOR TRACTOR CONTRACTOR FOR TRACTOR CONTRACTOR CONTRAC	
	1966-C	©CCCCGTCCCCGGGGACCAACCCGGCGCCCCCC		2027-C	CCCCCCCTCTCGGGGCGGCCCCCGTCCCC	
	2009-C	©CCCCCAATGGCCGGGCGTCCCAGGGGGAGGCAGGCCC		R149044-C	(CCCCCCGCCCCCGCGCGCCCCCCCCCCCCCCCCCCCC	
	2066-C	CCCCACGCCTTTCCCCTCCCC	ICP4	149088-C	CCCCGCGCTCCCGTTGGCCCCC	
ICP4	R146532-C	CCCACCCGCCCT _{CG} CGCCCCCCCCCCCCCCCCCCCCCCCCCC		149287-C	(CCCCCCCCCGACGCCCGCGCGTCCGC	
	146574-C	CCCGTTGGTCGAACCCCCGGCCCCCCCCC		R149570-C	COCCeCCCCCCCCCCCCCCCCCCCCCCCCCCCCCCCCC	
	146578-C	#CCCCGTCGCCCCCCCGTTCGTCGAACCCCCCCCCCCCCC	ICP22/ ICP47	132299-C	CCCCTCCCCCCCCCCCCCCCCCCCCCCCCCCCCCCCCC	
	146666-C	1000000 000000000000000000000000000000		132325-C	I_COOGTOODOOGGOOGTOOOGG	
	146947-C	CCCACGGACCCCGACGACCCCCGC		132988-C	CCCGCCCCCCGTCCGGGCCC	
	131746-C	CCCGGGCCCCGCCCCC_TGCCC	ICP27	114386-C	CONTOUND TO CONTOUR TO	
	R131803-C		ICF21	R114579-C	CCCCCTCGGAGGACACCCGCCATCCCAGCCCC	
	131857-C	CCCTTGGGCCGCCGCCGTCCCGTTGGTCC				
	132059-C	*COCCERCIAGE COCCERCIAGE COCCERCIACE COCCE				
ICP22/ ICP47	132065-C	CCCGCCCCCCCCCCCCCCCCCCCCCCCCCCCCCCCCCC	VZV (157 genomes)			
	132070-C	[CGCCGGAGAGACCCGCCCCCCGCCGCCCCCCCCCCCCC	ORF61	R104021-C	-COMMISSION THE COMMISSION FOR THE PROPERTY OF	
	R132290-C	CCCCCCCACCC	OKF61	105081-C	CCCGCCCGTCGCCCGCCC	
	132411-C			109246-C	CCCCCCCCTCGACCGCATATTTCCTCCCCC	
	132424-C		ORF62/ ORF63	109703-C	CCCGCCCACACCCCATAAAACCGC	
ICP27	113501-C	CCG CCCCCCGGGGGGCCCCCCGCCCCC		R110410-C	ECCCAATCGAAGGTCTCCCCCCCCCAATCCCCCATTCCCATTTTACCC	
	113519 C	CCCAAACCCCTCCTgGTTCCG CCCCCC	ORF4	4278-C	CCCCAAACAAGCTTACCTGCACCC	

Fig. 3. Conservation of PiMSs in α HHVs. Data were generated by aligning all virus genomes available in the NCBI databank, excluding those with biases, such incomplete sequencing or unassigned nucleotide stretches. The number of aligned genomes is reported for each virus. Consensus sequences are reported as WEBLOGO outputs visualizing the nucleotide frequency at each position across the aligned genomes: the Y-axis represents the conservation rate, ranging from 0 to 2, with higher values indicating greater conservation. Sequences showing sequencing issues are reported in black and the conservation ranges from 0 to 4.

sequence was classified as no-iM (HSV-2 ICPO 2027-C) (Figs. 5 and S2, Table S3).

Overall, PiMSs prediction and biophysical analyses revealed that all IE promoters in α HHVs, except for VZV ORF4 4278-C, harbor at least one highly conserved C-rich sequence capable of folding into an iM structure in vitro (Fig. 6). This finding underscores the potential biological significance of these structures in viral gene regulation.

3.3. iM and G4 folding during HSV-1 infection in human cells

We next evaluated the actual formation of iMs during a viral

infection in human cells. Concurrently, we investigated the presence of G4s in the complementary regions, which had previously been identified in vitro [10,21,46].

Among α HHVs, HSV-1 was chosen for cellular-level investigations due to its well-characterized infection cycle and significant relevance as a human pathogen [47,48]. To monitor the presence of both iMs and G4s in infected cells, we employed a CUT&Tag-qPCR method which was set up to recognize the HSV-1 genome. The technique provides high-resolution mapping of DNA structures at precise genomic locations [49], thus allowing us to assess iM and G4 folding in the virus genome at different time points after infection. iMab and BG4 antibodies were

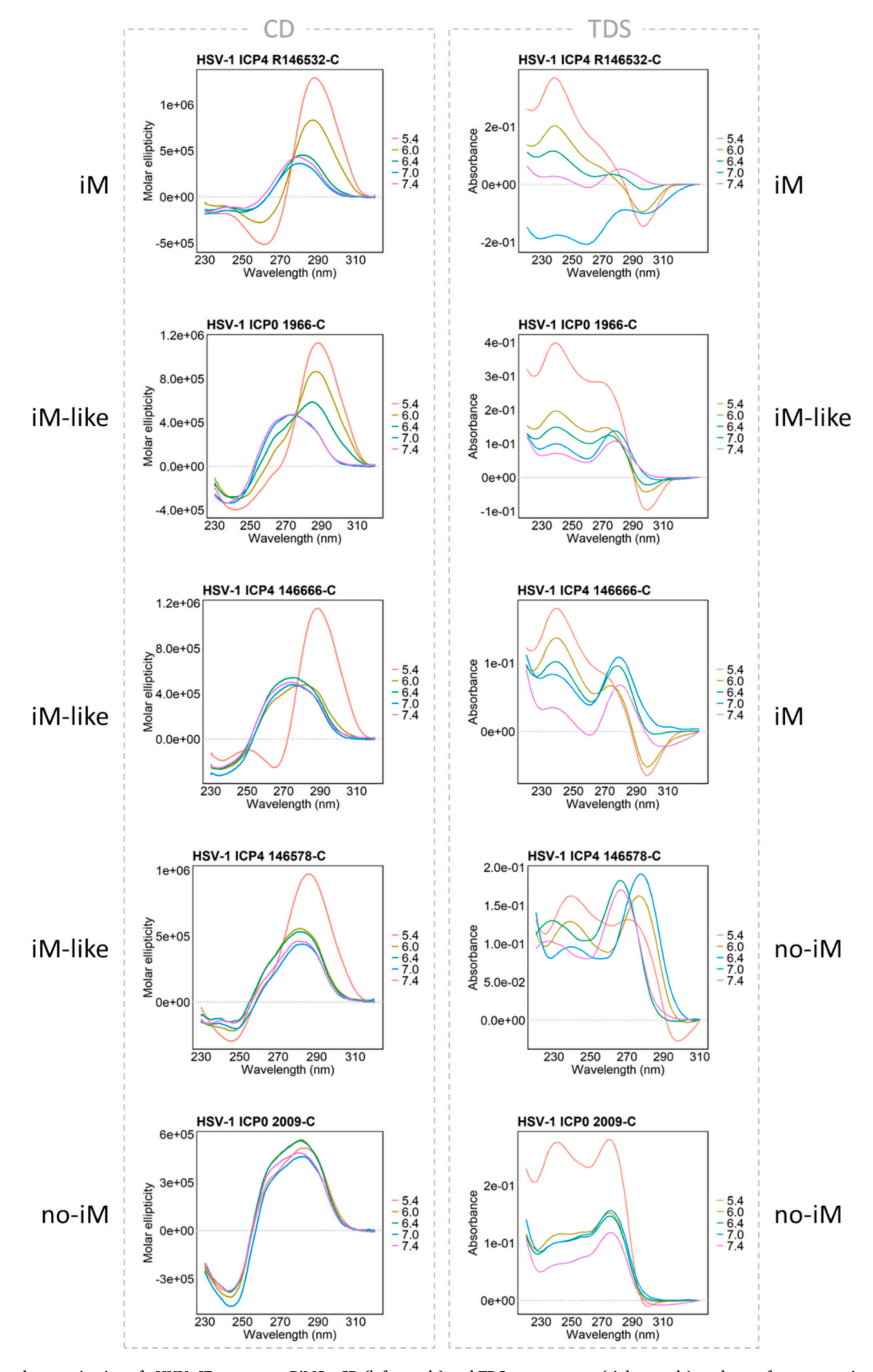


Fig. 4. Biophysics characterization of α HHVs IE promoters PiMSs. CD (left panels) and TDS spectroscopy (right panels) analyses of representative PiMSs reported in Table 1. Oligonucleotides were folded in phosphate buffer and analysed at different pH levels, as indicated. For each sequence, the formation of canonical iM (iM), iM-like structure (iM-like), or lack of characteristic folding (no-iM) is noted and reported in Table 1.

Table 1
PiMSs in αHHVs.

Promoter	Promoter length (bp)	Name	Sequence (5' - 3')	CD	TDS
HSV-1					
ICP0	~700	1875-C	CCCCAAAGAACCCCATTAGCATGCCCCTCCCGC	iM	iM
		1881-C	CCCGGTGTCCCCCAAAGAACCCCATTAGCATGCCCC	iM	iM
		1966-C	CCCCGTCCCCGGGGACCAACCCGGCGCCCCC	iM-like	iM-like
		2009-C	CCCCCAATGGCCGCGCTCCCAGGGGAGGCAGGCCC	no-iM	no-iM
		2066-C	CCCCACGCCTTTCCCCTCCCC	iM	iM
ICP4	~600	R146532-C	CCCACCCGCCCTCGCGCCCCCCCC	iM	iM
		146574-C	CCCGTTGGTCGAACCCCCGGCCCCCCCC	iM-like	iM
		146578-C	CCCGTGGCCGCGCCCGTTGGTCGAACCCCCGGCCCC	iM-like	no-iM
		146666-C	CCCCCGCCCCCGGCGGGCCCACCCC	iM-like	iM
		146947-C	CCCACGGACCCCGACGACCCCCGC	no-iM	no-iM
ICP22/ICP47	~1000	131746-C	CCCGGGCCCCGCCCCTGCCC	iM-like	iM
		R131803-C	CCCCGCGCGCCCGTTGGCCGTCCCCGGGCCCCCCGGTCCCGCCC	iM	iM
		131857-C	CCCTTGGGCCGCCGCCGTCCCGTTGGTCCC	iM-like	iM
		132059-C	CGCCGGAGAGACCCGCCCCCCCGCCCGCCCGGCCCCCCCC	iM-like	iM
		132065-C	CCCGCCCCCGCCGCCCGGGCCC	iM-like	iM
		132070-C	CGCCGGAGACCCGCCCCCCGCCGCCCC	iM-like	iM
		R132290-C	CCCGCCCACCCCCCCC	iM	iM
		132411-C	CCCCTCCTCCGCCCCGCGTCCCCCCTCCTCCGCCCCC	iM	iM
		132424-C	CCCCCGCGTCCCCCCTCCTCCGCCCCCCGCGTCCCCCCC	iM	iM
ICP27	~280	113501-C	CCGCCCCCGGGCGGGGCCCCCCCCCCCCCCCCCCCCCCC	no-iM	no-iM
101 27	~280	113501-C	CCCAAACCCCTCCTCGTTCCGCCCCCC	iM	iM
HSV-2					
ICP0	~800	R1571-C	CCCGGACTCCGCCCGGCGACCGCCCCGCGCCGCGCTTCCC	iM	iM
		1913-C	CCCCCGGCGCCCGGCGCGCGCCTGAGTGGTGCCCGCCCCC	iM-like	iM
		2027-C	CCCCCCTCTCGGGGCGCCCCGTCCCC	iM-like	iM
ICP4	~1000	R149044-C	CCCCCGCCCCGCGCCCCC	iM	iM
		149088-C	CCCCGCGCTCCCGTTGGCCCCCGCCGGCCCC	iM	iM
		149287-C	CCCCGCCCGACGCCCGCGCGTCCGC	iM-like	iM
		R149570-C	CCACCCCCCCACTGCCGCCCC	iM	iM
ICP22/ICP47	~1000	132299-C	CCCGTCCCCCGGCCCGGCCCCCC	iM-like	iM
		132325-C	CCCGTCCCCCGGCCCGTCCCCCC	iM-like	iM
		132988-C	CCCGCCCCCGTCCGGGCCC	iM-like	iM
ICP27	~250	114386-C	CCCTCCCCGTCGGGCGTCACCGCCCCCGCCCCCGCC	iM	iM
			GTCCCC		
		R114579-C	CCCCCTCGGAGGACACCCGCCATCCCAGCCCC	iM-like	iM
VZV					
ORF61	~630	R104021-C	CCCCCCCGAAAATAACCCCCCCGGTTTCTGGGCGCCCGGCGGACCCC	iM-like	iM
ORTOI	030	105081-C	CCCGCCCGTAAATAACCCCCCCGGTTTCTGGGCGCCCGGCGGACCCC	iM-iike	iM
OPEG2/	~1000	109246-C		iM-like	iM
ORF62/ ORF63	~1000		CCCCCCCTCGACCGCATAAAACCCC		
		109703-C	CCCGCCCACACCCCATAAAACCGC	iM-like	iM-like
ODEA	170	R110410-C	CCCAATCGAAGGTCTCCCGCCCCGGAATCCCCCATTGCCATTTTACCC	iM-like	iM
ORF4	~170	4278-C	CCCCAAACAAGCTTACCTGCACCC	no-iM	no-iM

PiMSs are identified by their 3' nucleotide positions on the respective viral genomes (NC_001806.2 for HSV-1; NC_001798.2 for HSV-2; and NC_001348.1 for VZV). PiMSs are located on the lagging strand, except those with an "R" prefix in the "Name" that are on the reverse (leading) strand. For each promoter, the length in bases is indicated. Results from CD and TDS analyses are reported: 'iM' indicates positive iM folding, 'no-iM' indicates the absence of iM folding and 'iM-like' indicates dynamic folding with mixed features.

utilized as previously described [27,31,37] to map iMs and G4s, respectively, at two key time points of the HSV-1 viral cycle: the initial phase of viral transcription (1 hpi) and the early onset of viral replication (4 hpi) [47].

Our results showed that iMs do form within HSV-1 IE promoters in infected cells. Additionally, we also confirmed that G4s are folded in the same promoters (Fig. 7A-B). The enrichment of both iMs and G4s increased over time for all IE genes from 1 hpi to 4 hpi, which was accompanied by increased gene expression (see Fig. 7C). ICP4 displayed the lowest signal in both iMs and G4s folding over time and was also the least expressed among IE genes.

Notably, these findings represent the first evidence of the presence of both iMs and G4s in a viral genome, specifically the HSV-1 IE promoters, during different stages of viral infection, revealing dynamic changes in their enrichment levels over time. The observed variations suggest that these non-canonical DNA structures may contribute to the regulation of viral gene expression.

4. Discussion

The presence of both iMs and G4s in viral promoters is an unexplored aspect of virus gene regulation. While G4s are emerging as key modulators of viral transcription, fine-tuning viral gene expression, the presence and biological role of iMs in viral genomes are still unexplored.

By integrating motif predictions, biophysical and in cell analysis, we provide the first evidence that i) α HHVs IE promoters contain highly conserved PiMSs; ii) in each IE promoter, except for VZV ORF4 4278-C, at least one PiMS folds into iM in vitro; iii) iMs and G4s are folded in the viral genome during infection in human cells and their formation is associated with changes in gene expression, supporting their potential role in viral gene regulation.

The remarkably high conservation rate of the selected iMs across multiple viral isolates underscores their potential functional significance. Notably, this conservation extends beyond the C-tracts, which are essential for iM formation, to encompass the loop sequences that influence folding dynamics and stability. The consistent maintenance of both C-tracts and loops suggests that iMs in $\alpha HHVs$ may serve as critical

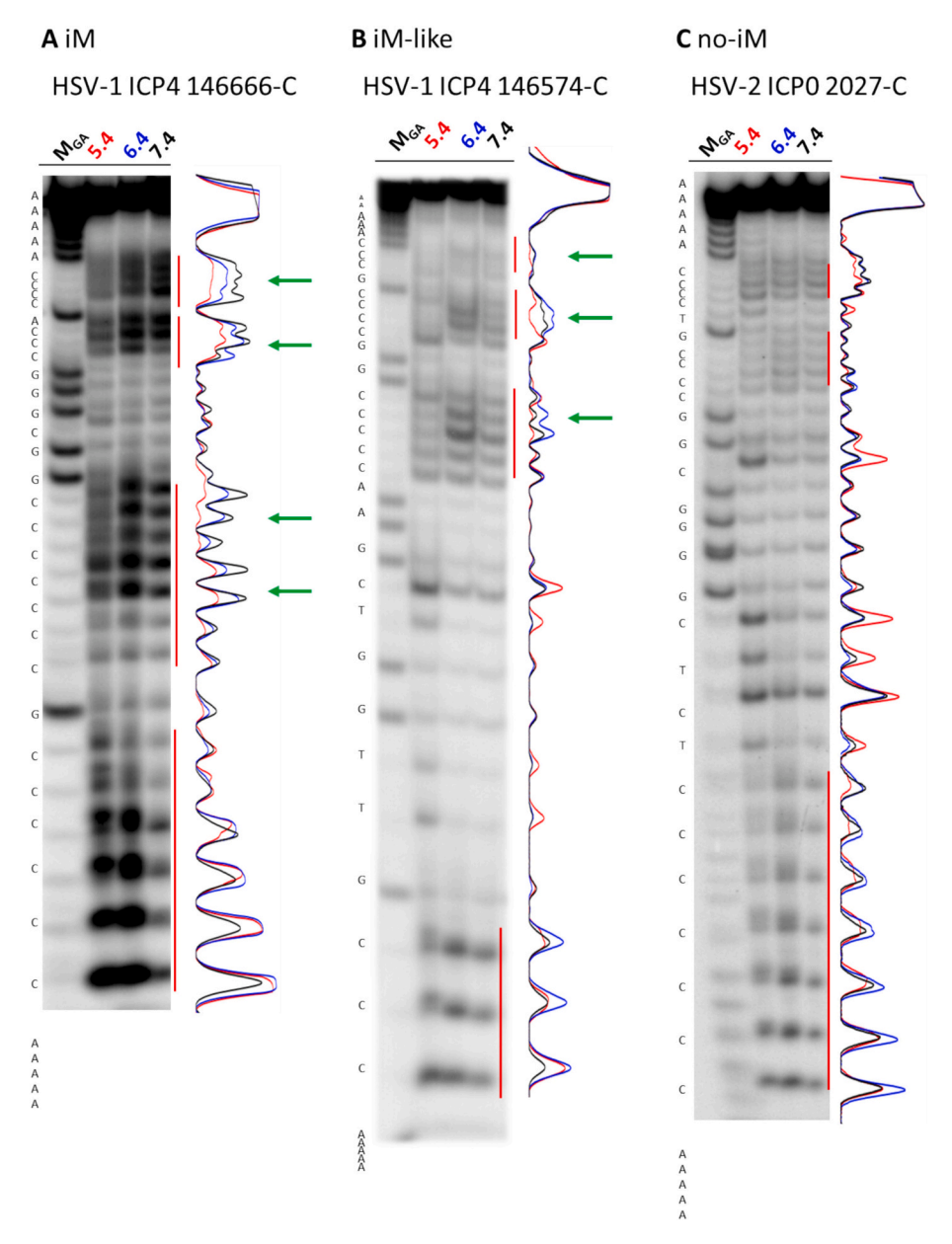


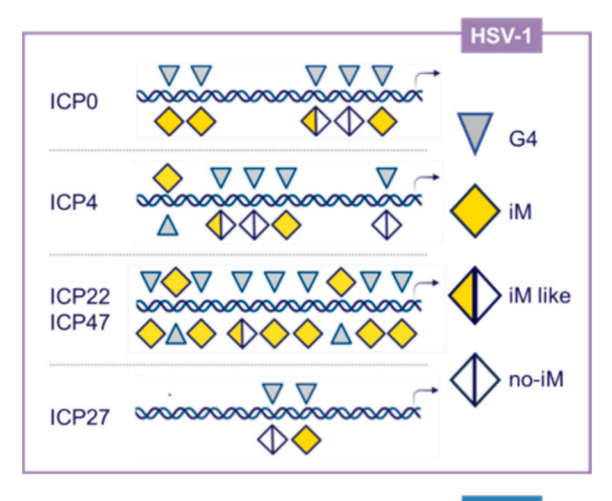
Fig. 5. Bromine footprinting protection assay of representative α HHVs PiMSs. HSV-1 ICP4-R146666-C (A) and ICP4 146574-C (B) and HSV-2 ICP0 2027-C (C) oligonucleotides (5 pmol) were folded in phosphate buffer 20 mM at the indicated pH values, in the presence of KCl 80 mM. M is a marker lane obtained with the Maxam and Gilbert sequencing protocol. Densitograms show quantification of cleaved bands intensity at different pH levels: pH 5.4 red line; pH 6.0 blue line and pH 7.4 black line. Green arrows indicate protected C-tracts, red lines indicate C-tracts.

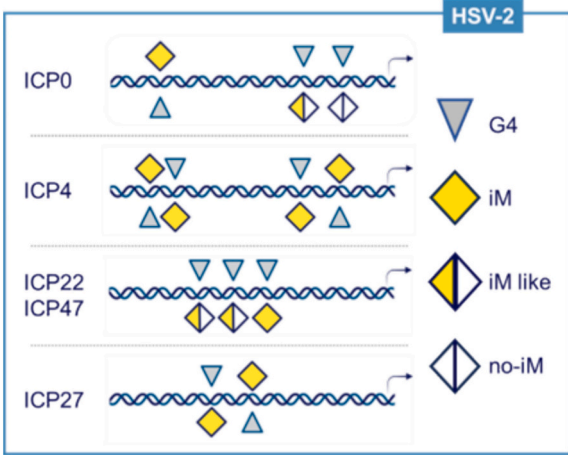
protein binding sites or other functional domains within these regions [50].

Investigation of iMs across α HHVs IEs revealed distinct patterns among HSV-1, HSV-2 and VZV, suggesting virus-specific regulatory adaptations. HSV-1 contains the highest number of iMs, which aligns with its G4 profile [21]. In contrast, despite its high homology with HSV-1, HSV-2 shows a more variable pattern. In contrast, VZV harbors significantly fewer iMs, likely due to its distinct infectious cycle and genomic composition [51]. The ICP22/ICP47 promoter, the longest in both HSV-1 and HSV-2, harbors the highest number of iMs. Given their proximity to one of the three viral replication origins (OriS), these iMs may play a dual role in coordinating transcription and replication [52]. Similarly, the ICP4 promoter, which encodes the main viral transcription regulator and is also adjacent to an OriS, contains numerous iMs [52]. The ICP0 promoter, responsible for indirect transcription promotion, also exhibits a high number of iMs, indicating possible structure-

related expression control [53]. In contrast, the ICP27 promoter, encoding a protein crucial for RNA polymerase recruitment and viral RNA export, shows minimal iM presence, possibly reflecting its continuous expression throughout the viral cycle [54,55]. In VZV, while IE genes generally demonstrated limited iM presence, the ORF62/ORF63 promoters flanking the OriS contain the highest number of iMs [56], similarly to Simplexviruses. This heterogeneity in iM occurrence across viruses and promoters (Fig. 6) suggests specialized regulatory roles for each gene. The higher prevalence and structural uniformity of iMs in HSV-1 suggest a more stable regulatory role, whereas HSV-2 greater diversity may confer adaptive flexibility. VZV limited and structurally distinct iMs further emphasize its unique viral life cycle and host interactions.

To improve our understanding of the presence of iMs in α HHV IE promoters, we combined the results of several biophysical analyses, emphasising the importance of using multiple spectroscopic techniques





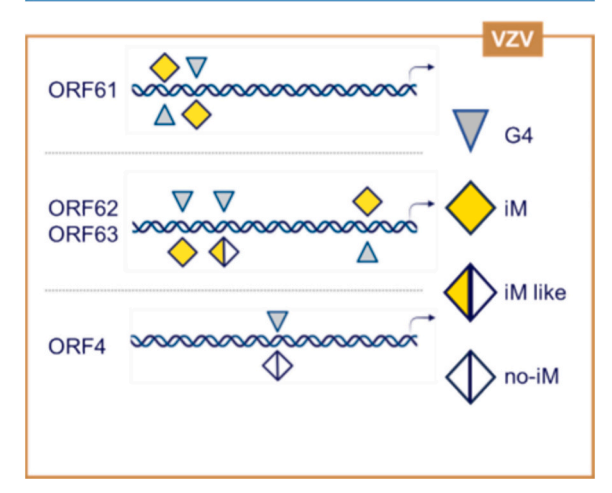


Fig. 6. Scheme showing the PiMSs identified in the α HHVs IE promoters. Rotated squares indicate PiMSs categorized by in vitro analysis as iM (solid yellow), iM-like structures (half yellow, half white), and non-iM (white). Grey triangles indicate previously characterized G4s, identified on the strand complementary to iMs.

to study iM folding dynamics and stability [41,57]. This study indeed shows the presence of iM-like structures that may be overlooked in initial biophysical analyses, but which can be characterized more effectively using the bromine footprinting protection assay [32,58]. We were able to identify the C residues involved in iM structural bonds, revealing sequences that fold into incomplete iMs, even when all sequence characteristics for complete iM formation are present. These iM-like structures may require protein binding to complete their folding,

suggesting the presence of a higher level of regulatory control by iMs in the cellular environment. Notably, HSV-1 ICPO 2027-C sequence showed three different results, further confirming the complexity of iM formation.

This analysis further demonstrated that not all genomic regions that form G4 structures on one strand harbor an iM on the opposite strand. This supports the idea that, also in viral genomes, the two secondary structures have distinct folding dynamics and are involved in different regulatory mechanisms [30,31]. As already observed for G4s, iMs in $\alpha HHVs$ do not strictly adhere to the rules established for human iM folding [21,59]. Sequences with C-tracts composed of three to five Cs (e. g., 132424-C in HSV-1 ICP22/ICP47 promoter) tend to better fold into iMs, aligning with data regarding iM regions within the human genome [25]. By contrast, long C-tracts and additional C-islands (spare tires), which generally stabilize iMs [60], produced inconsistent results, strengthening folding in some cases (e.g., R131803-C in HSV-1 ICP22/ ICP47 promoter) but destabilizing in others (e.g., 132059-C in HSV-1 ICP22/ICP47 promoter). These contrasting outcomes suggest that additional sequence features contribute to folding behaviour. Loop length and composition also emerged as a key determinant of αHHV iM behaviour in IE promoters. iMs fold more readily when an alternating pattern of short and long loops is present (e.g., 114386-C in HSV-2 ICP27 promoter), suggesting that loop balance plays an important role in structural dynamics. Regression models further support that longer Ctracts and shorter loops favour stability [61-63]. In this complex scenario, it cannot be excluded that very short loops may instead hinder proper folding, as observed for HSV-2 ICP4 R149044-C and VZV ORF61 105081-C, where positive spectroscopic signals may also reflect intermolecular rather than intramolecular assemblies. In our investigations, many loop sequences were found to be highly enriched in GC content (Fig. 2), which may influence the folding dynamics and enhance iM stability through additional Watson and Crick base pairing [64]. Conversely, AT-rich loops hinder folding or destabilize the iM structure, resulting in more dynamic and iM-like structures (e.g., R104021-C in VZV ORF61 promoter). It should be noted that we retrieved a limited number of AT-rich loops, due to the genomic characteristics of these viruses, which are extremely GC-rich, and that the AT-rich tracts are often embedded in long loops, another factor not favoring iM folding [65]. Importantly, iMs do not tolerate the presence of nucleotides creating bulges within the C-tracts, unlike G4s.

Our data indicate that HSV-1 favours regular iMs with C-tracts consisting of three or four Cs, as well as medium length and/or short loops. HSV-2 showed the same abundance of confirmed iM structures, despite differences in PiMS composition, as it can accommodate iMs with either a one-nucleotide loop or longer loops. This suggests that despite being homologous, these two viruses may have evolved different strategies for regulating transcription [4,66]. VZV exhibits a different approach to iMs, seemingly able to take advantage of long C-tracts interspersed in long loops (e.g., R104021-C in ORF61 promoters), further highlighting its difference from the other two αHHVs.

Our findings underscore that iM formation cannot be reliably predicted solely from primary sequence analysis or biophysical assays. The cellular environment introduces complex factors influencing iM formation, such as local pH fluctuations, molecular crowding, epigenetic modifications, and protein interactions [25,67]. This complexity means that sequences not forming iMs in vitro may still occur within cells. Therefore, a comprehensive approach combining in silico predictions with both in vitro and in cell experimental validations is crucial for accurately monitoring iM formation.

To this end, we assessed iM and G4 folding in α HHV promoters across different stages of virus infection in human cells. Our results demonstrate that both iMs and G4s can form within the same regulatory regions; however, it is not possible to determine whether their folding occurs in the exact position, as the same region embeds multiple GC-rich sequences. Nonetheless, this observation suggests a previously unrecognized layer of transcriptional modulation in α HHV genomes. The

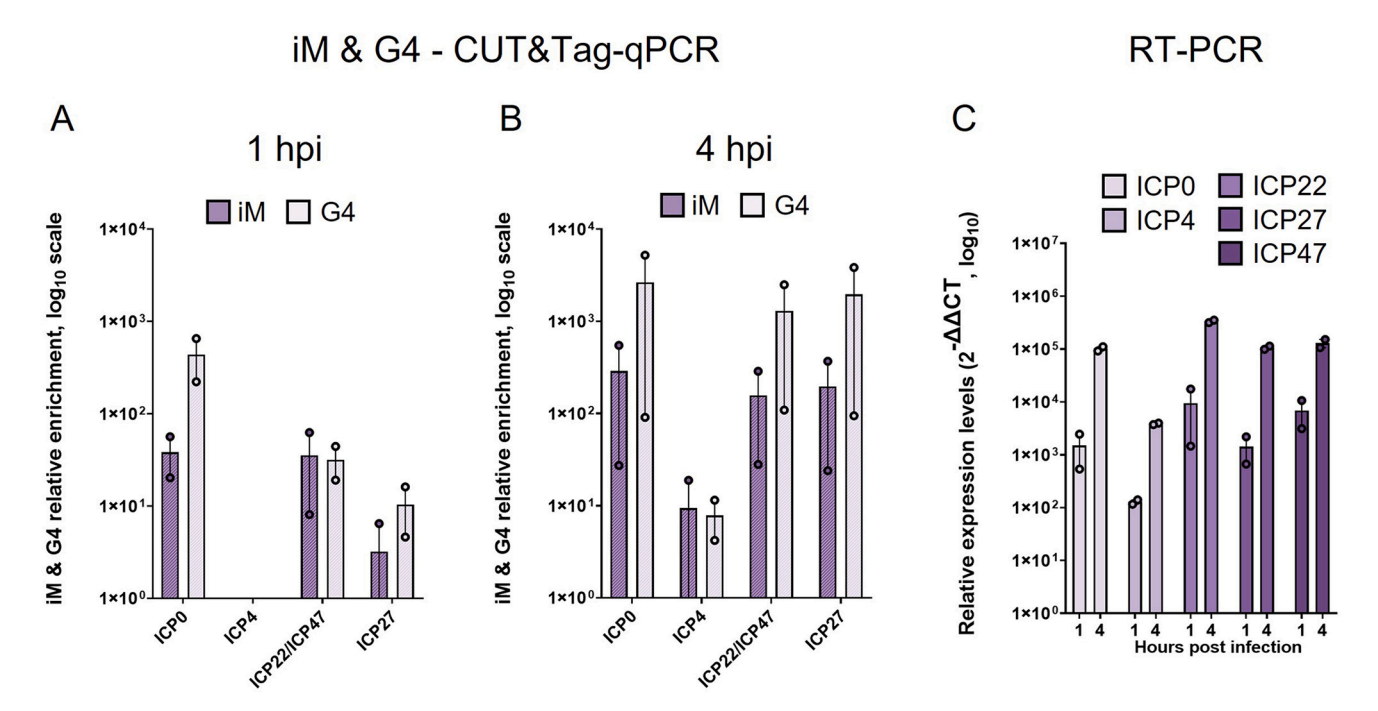


Fig. 7. iM and G4 folding in HSV-1 IE promoters during HSV-1 infection in human cells. iMab- and BG4-CUT&Tag was performed on U-2 OS cells infected with HSV-1 at MOI = 2 and collected at 1 (A) and 4 (B) hpi, followed by qPCR analysis. Data have been normalized on IgG signal. The relative IE gene expression (C) was assessed by qPCR using the same infection model as for the CUT&Tag experiment. Bar graphs represent the mean \pm SEM (error bars) from two biological replicates, indicated by dots.

enrichment of both structures varies across the tested genes, with G4s appearing slightly more abundant. This difference may be due to a suboptimal ability of the iMab antibody to recognize iM-like structures, as it primarily recognizes well-folded and stable intra- and intermolecular iMs [27].

Additionally, the variations in iM and G4 folding could reflect the well-documented difference in thermodynamic stability between G4s and iMs, particularly under physiological conditions. Notably, iMs can be stabilized by adjacent complementary G4s, also at the chromatin level [31,68], which may be the case in IE promoters, where iM enrichment was consistently observed (Fig. 7A-B). Except for ICP4, we observed both iMs and G4s at different phases of viral infection, likely due to the capacity of these promoters to harbor multiple structures in their sequences. As a result, a dynamic equilibrium of iMs and G4s manifesting at different times emerges, indicating that as viral transcription intensifies, both structures fold. In this intricate environment, it remains unclear whether G4s and iMs are both enhancing viral transcription, or if they serve as a viral mechanism to fine-tune transcription. It is important to note that while our results show a correlation between increased formation of both G4s and iMs and transcription levels, we cannot determine whether both or just one of the two structures is responsible for this effect. The interplay between G4s and iMs might involve complex cooperative or competitive mechanisms that collectively influence transcription, necessitating more detailed quantitative analyses to fully understand their roles. Regarding ICP4, our and other groups have established that its promoter is tightly regulated, with ICP4 itself strongly binding to its own promoter to control its activity [10,69,70]. This intense protein coverage may explain the absence of detectable G4 signals from that region. Additionally, the unique behaviour of the ICP4 promoter underscores the complexity of regulatory mechanisms in viral genomes and highlights the need for promoterspecific analyses when studying the roles of non-canonical DNA structures in transcriptional regulation.

5. Conclusion

This study reveals the presence of both iMs and G4s in viral promoter regions, thereby expanding our understanding of DNA secondary structures in viral infections. Genome-wide studies in an infected cellular context will be needed to elucidate the effect of iM and G4 folding dynamics on host chromatin and viral genome architectures. While iMs are recognized as potential therapeutic targets for diseases such as cancer and neurological disorders [25,71], our work demonstrates their presence at the viral level as well. This finding suggests the possibility of targeting these structures in innovative antiviral therapies.

CRediT authorship contribution statement

Emanuela Ruggiero: Writing – review & editing, Writing – original draft, Validation, Investigation, Formal analysis, Data curation. Filippo Mattellone: Investigation. Daniel Christ: Writing – review & editing, Supervision. Sara N. Richter: Writing – review & editing, Supervision, Funding acquisition, Conceptualization. Ilaria Frasson: Writing – review & editing, Writing – original draft, Validation, Supervision, Investigation, Funding acquisition, Formal analysis, Data curation, Conceptualization.

Declaration of competing interest

The authors declare that they have no known competing financial interests or personal relationships that could have appeared to influence the work reported in this paper.

Acknowledgments

This work was funded by the Department of Molecular Medicine of the University of Padova to I.F. and S.N.R.

Appendix A. Supplementary data

Supplementary data to this article can be found online at https://doi.org/10.1016/j.jjbiomac.2025.148464.

Data availability

Data will be made available on request.

References

- Herpes simplex virus, (n.d.). https://www.who.int/news-room/fact-sheets/detail/ herpes-simplex-virus (accessed July 2, 2025).
- [2] B.N. Fields, D.M. Knipe, P.M. Howley, Fields Virology, 6th ed., Wolters Kluwer Health/Lippincott Williams & Wilkins, Philadelphia, 2013.
- [3] L. Djakovic, T. Hennig, K. Reinisch, A. Milić, A.W. Whisnant, K. Wolf, E. Weiß, T. Haas, A. Grothey, C.S. Jürges, M. Kluge, E. Wolf, F. Erhard, C.C. Friedel, L. Dölken, The HSV-1 ICP22 protein selectively impairs histone repositioning upon Pol II transcription downstream of genes, Nat. Commun. 14 (2023) 4591, https://doi.org/10.1038/s41467-023-40217-w.
- [4] L.E.M. Dunn, C.H. Birkenheuer, R. Dufour, J.D. Baines, Immediate early proteins of herpes simplex virus transiently repress viral transcription before subsequent activation, J. Virol. 96 (2022) e0141622, https://doi.org/10.1128/jvi.01416-22.
- [5] X. Wang, T. Hennig, A.W. Whisnant, F. Erhard, B.K. Prusty, C.C. Friedel, E. Forouzmand, W. Hu, L. Erber, Y. Chen, R.M. Sandri-Goldin, L. Dölken, Y. Shi, Herpes simplex virus blocks host transcription termination via the bimodal activities of ICP27, Nat. Commun. 11 (2020) 293, https://doi.org/10.1038/ s41467-019-14109-x.
- [6] L.E.M. Dunn, J.D. Baines, Herpes simplex virus 1 immediate early transcription initiation, pause-release, elongation, and termination in the presence and absence of ICP4, J. Virol. 97 (2023) e0096023, https://doi.org/10.1128/jvi.00960-23.
- [7] L.E.M. Dunn, C.H. Birkenheuer, J.D. Baines, A revision of herpes simplex virus type 1 transcription: first, repress; then, express, Microorganisms 12 (2024) 262, https://doi.org/10.3390/microorganisms12020262.
- [8] S.E. Dremel, N.A. DeLuca, Herpes simplex viral nucleoprotein creates a competitive transcriptional environment facilitating robust viral transcription and host shut off, eLife 8 (2019) e51109, https://doi.org/10.7554/eLife.51109.
- [9] B. Grondin, N. DeLuca, Herpes simplex virus type 1 ICP4 promotes transcription preinitiation complex formation by enhancing the binding of TFIID to DNA, J. Virol. 74 (2000) 11504–11510.
- [10] I. Frasson, P. Soldà, M. Nadai, S. Lago, S.N. Richter, Parallel G-quadruplexes recruit the HSV-1 transcription factor ICP4 to promote viral transcription in herpes virusinfected human cells, Commun. Biol. 4 (2021) 510, https://doi.org/10.1038/ s42003-021-02035-y
- [11] R. Hänsel-Hertsch, M. Di Antonio, S. Balasubramanian, DNA G-quadruplexes in the human genome: detection, functions and therapeutic potential, Nat. Rev. Mol. Cell Biol. 18 (2017) 279–284, https://doi.org/10.1038/nrm.2017.3.
- [12] F. Wu, K. Niu, Y. Cui, C. Li, M. Lyu, Y. Ren, Y. Chen, H. Deng, L. Huang, S. Zheng, L. Liu, J. Wang, Q. Song, H. Xiang, Q. Feng, Genome-wide analysis of DNA Gquadruplex motifs across 37 species provides insights into G4 evolution, Commun. Biol. 4 (2021) 1–11, https://doi.org/10.1038/s42003-020-01643-4.
- [13] D. Varshney, J. Spiegel, K. Zyner, D. Tannahill, S. Balasubramanian, The regulation and functions of DNA and RNA G-quadruplexes, Nat. Rev. Mol. Cell Biol. 21 (2020) 459–474, https://doi.org/10.1038/s41580-020-0236-x.
- [14] E. Ruggiero, S.N. Richter, G-Quadruplexes, Human Viruses: A Promising Route to Innovative Antiviral Therapies, in: Handb. Chem. Biol. Nucleic Acids, Springer, Singapore, 2023, pp. 2465–2492, https://doi.org/10.1007/978-981-19-9776-1_81.
- [15] E. Ruggiero, M. Tassinari, R. Perrone, M. Nadai, S.N. Richter, Stable and conserved G-Quadruplexes in the long terminal repeat promoter of retroviruses, ACS Infect. Dis. 5 (2019) 1150–1159, https://doi.org/10.1021/acsinfecdis.9b00011.
- [16] R. Perrone, E. Lavezzo, G. Palù, S.N. Richter, Conserved presence of G-quadruplex forming sequences in the long terminal repeat promoter of lentiviruses, Sci. Rep. 7 (2017) 2018, https://doi.org/10.1038/s41598-017-02291-1.
- [17] R. Perrone, M. Nadai, I. Frasson, J.A. Poe, E. Butovskaya, T.E. Smithgall, M. Palumbo, G. Palù, S.N. Richter, A dynamic G-quadruplex region regulates the HIV-1 long terminal repeat promoter, J. Med. Chem. 56 (2013) 6521–6530, https://doi.org/10.1021/jm400914r.
- [18] A. De Rache, J. Marquevielle, S. Bouaziz, B. Vialet, M.-L. Andreola, J.-L. Mergny, S. Amrane, Structure of a DNA G-quadruplex that modulates SP1 binding sites architecture in HIV-1 promoter, J. Mol. Biol. 436 (2024) 168359, https://doi.org/ 10.1016/j.jmb.2023.168359.
- [19] G. Nicoletto, S.N. Richter, I. Frasson, Presence, location and conservation of putative G-Quadruplex forming sequences in arboviruses infecting humans, Int. J. Mol. Sci. 24 (2023) 9523, https://doi.org/10.3390/ijms24119523.
- [20] P. Schult, B.M. Kümmerer, M. Hafner, K. Paeschke, Viral hijacking of hnRNPH1 unveils a G-quadruplex-driven mechanism of stress control, Cell Host Microbe 32 (2024) 1579–1593.e8, https://doi.org/10.1016/j.chom.2024.07.006.
- [21] I. Frasson, M. Nadai, S.N. Richter, Conserved G-quadruplexes regulate the immediate early promoters of human alphaherpesviruses, Mol. Basel Switz. 24 (2019) 2375, https://doi.org/10.3390/molecules24132375.
- [22] S. Artusi, R. Perrone, S. Lago, P. Raffa, E. Di Iorio, G. Palù, S.N. Richter, Visualization of DNA G-quadruplexes in herpes simplex virus 1-infected cells,

- Nucleic Acids Res. 44 (2016) 10343–10353, https://doi.org/10.1093/nar/gkw968.
- [23] S. Artusi, M. Nadai, R. Perrone, M.A. Biasolo, G. Palù, L. Flamand, A. Calistri, S. N. Richter, The herpes simplex Virus-1 genome contains multiple clusters of repeated G-quadruplex: implications for the antiviral activity of a G-quadruplex ligand, Antiviral Res. 118 (2015) 123–131, https://doi.org/10.1016/j.antiviral.2015.03.016
- [24] B. Dauber, H.A. Saffran, J.R. Smiley, The herpes simplex virus 1 Virion host shutoff protein enhances translation of viral late mRNAs by preventing mRNA overload, J. Virol. 88 (2014) 9624–9632, https://doi.org/10.1128/JVI.01350-14.
- [25] S. Tao, Y. Run, D. Monchaud, W. Zhang, i-motif DNA: identification, formation, and cellular functions, trends genet, TIG 40 (2024) 853–867, https://doi.org/ 10.1016/j.tig.2024.05.011.
- [26] C.D. Peña Martinez, M. Zeraati, R. Rouet, O. Mazigi, J.Y. Henry, B. Gloss, J. A. Kretzmann, C.W. Evans, E. Ruggiero, I. Zanin, M. Marušič, J. Plavec, S. N. Richter, T.M. Bryan, N.M. Smith, M.E. Dinger, S. Kummerfeld, D. Christ, Human genomic DNA is widely interspersed with i-motif structures, EMBO J. 43 (2024) 4786–4804, https://doi.org/10.1038/s44318-024-00210-5.
- [27] E. Ruggiero, M. Marušič, I. Zanin, C.D. Peña Martinez, D. Christ, J. Plavec, S. N. Richter, The iMab antibody selectively binds to intramolecular and intermolecular i-motif structures, Nucleic Acids Res. 53 (2025) gkae1305, https://doi.org/10.1093/nar/gkae1305.
- [28] M. Zeraati, D.B. Langley, P. Schofield, A.L. Moye, R. Rouet, W.E. Hughes, T. M. Bryan, M.E. Dinger, D. Christ, I-motif DNA structures are formed in the nuclei of human cells, Nat. Chem. 10 (2018) 631–637, https://doi.org/10.1038/s41557-018-0046-3.
- [29] D. Guneri, E. Alexandrou, K. El Omari, Z. Dvořáková, R.V. Chikhale, D.T.S. Pike, C. A. Waudby, C.J. Morris, S. Haider, G.N. Parkinson, Z.A.E. Waller, Structural insights into i-motif DNA structures in sequences from the insulin-linked polymorphic region, Nat. Commun. 15 (2024) 7119, https://doi.org/10.1038/s41467-024-50553-0.
- [30] J.J. King, K.L. Irving, C.W. Evans, R.V. Chikhale, R. Becker, C.J. Morris, C.D. Peña Martinez, P. Schofield, D. Christ, L.H. Hurley, Z.A.E. Waller, K.S. Iyer, N.M. Smith, DNA G-Quadruplex and i-motif structure formation is interdependent in human cells, J. Am. Chem. Soc. 142 (2020) 20600–20604, https://doi.org/10.1021/ jacs.0c11708.
- [31] I. Zanin, E. Ruggiero, G. Nicoletto, S. Lago, I. Maurizio, I. Gallina, S.N. Richter, Genome-wide mapping of i-motifs reveals their association with transcription regulation in live human cells, Nucleic Acids Res. 51 (2023) 8309–8321, https://doi.org/10.1093/nar/gkad626.
- [32] E. Ruggiero, S. Lago, P. Šket, M. Nadai, I. Frasson, J. Plavec, S.N. Richter, A dynamic i-motif with a duplex stem-loop in the long terminal repeat promoter of the HIV-1 proviral genome modulates viral transcription, Nucleic Acids Res. 47 (2019) 11057–11068, https://doi.org/10.1093/nar/gkz937.
- [33] O. Kikin, L. D'Antonio, P.S. Bagga, QGRS mapper: a web-based server for predicting G-quadruplexes in nucleotide sequences, Nucleic Acids Res. 34 (2006) W676–W682, https://doi.org/10.1093/nar/gkl253.
- [34] P. Dhapola, S. Chowdhury, QuadBase2: web server for multiplexed guanine quadruplex mining and visualization, Nucleic Acids Res. 44 (2016) W277–W283, https://doi.org/10.1093/nar/gkw425.
- [35] G.E. Crooks, G. Hon, J.-M. Chandonia, S.E. Brenner, WebLogo: a sequence logo generator, Genome Res. 14 (2004) 1188–1190, https://doi.org/10.1101/ gr.849004.
- [36] A.M. Maxam, W. Gilbert, [57] sequencing end-labeled DNA with base-specific chemical cleavages, Methods Enzymol. (1980) 499–560, https://doi.org/10.1016/ S0076-6879(80)65059-9
- [37] I. Maurizio, B. Tosoni, I. Gallina, E. Ruggiero, I. Zanin, S.N. Richter, Chapter nine-production of the anti-G-quadruplex antibody BG4 for efficient genome-wide analyses: From plasmid quality control to antibody validation, in: K.D. Raney, R. L. Eoff, A.K. Byrd, S. Kendrick (Eds.), Methods Enzymol., Academic Press, 2024, pp. 193–219, https://doi.org/10.1016/bs.mie.2023.11.004.
 [38] J.D. Buenrostro, B. Wu, U.M. Litzenburger, D. Ruff, M.L. Gonzales, M.P. Snyder, H.
- [38] J.D. Buenrostro, B. Wu, U.M. Litzenburger, D. Ruff, M.L. Gonzales, M.P. Snyder, H. Y. Chang, W.J. Greenleaf, Single-cell chromatin accessibility reveals principles of regulatory variation, Nature 523 (2015) 486–490, https://doi.org/10.1038/nature14590
- [39] K.J. Livak, T.D. Schmittgen, Analysis of relative gene expression data using real-time quantitative PCR and the 2(-Delta Delta C(T)) method, Methods San Diego Calif 25 (2001) 402–408, https://doi.org/10.1006/meth.2001.1262.
- [40] Y. Luo, A. Granzhan, J. Marquevielle, A. Cucchiarini, L. Lacroix, S. Amrane, D. Verga, J.-L. Mergny, Guidelines for G-quadruplexes: I. *In vitro* characterization, Biochimie. 214 (2023) 5–23, https://doi.org/10.1016/ji.biochi.2022.12.019.
- [41] N. Iaccarino, M. Cheng, D. Qiu, B. Pagano, J. Amato, A. Di Porzio, J. Zhou, A. Randazzo, J.-L. Mergny, Effects of sequence and base composition on the CD and TDS profiles of i-DNA, Angew. Chem. Int. Ed. Engl. 60 (2021) 10295–10303, https://doi.org/10.1002/anie.202016822.
- [42] E.P. Wright, J.L. Huppert, Z.A.E. Waller, Identification of multiple genomic DNA sequences which form i-motif structures at neutral pH, Nucleic Acids Res. 45 (2017) 2951–2959, https://doi.org/10.1093/nar/gkx090.
- [43] M. Cheng, D. Qiu, L. Tamon, E. Ištvánková, P. Víšková, S. Amrane, A. Guédin, J. Chen, L. Lacroix, H. Ju, L. Trantírek, A.B. Sahakyan, J. Zhou, J.-L. Mergny, Thermal and pH stabilities of i-DNA: confronting in vitro experiments with models and in-cell NMR data, Angew. Chem. Int. Ed. 60 (2021) 10286–10294, https://doi.org/10.1002/anie.202016801.
- [44] J. Kypr, I. Kejnovská, D. Renciuk, M. Vorlícková, Circular dichroism and conformational polymorphism of DNA, Nucleic Acids Res. 37 (2009) 1713–1725, https://doi.org/10.1093/nar/gkp026.

- [45] A. Garabedian, D. Butcher, J.L. Lippens, J. Miksovska, P.P. Chapagain, D. Fabris, M.E. Ridgeway, M.A. Park, F. Fernandez-Lima, Structures of the kinetically trapped i-motif DNA intermediates, Phys. Chem. Chem. Phys. 18 (2016) 26691–26702, https://doi.org/10.1039/C6CP04418B.
- [46] I. Frasson, P. Soldà, M. Nadai, M. Tassinari, M. Scalabrin, V. Gokhale, L.H. Hurley, S.N. Richter, Quindoline-derivatives display potent G-quadruplex-mediated antiviral activity against herpes simplex virus 1, Antiviral Res. 208 (2022) 105432, https://doi.org/10.1016/j.antiviral.2022.105432.
- [47] M.K. Pietilä, J.J. Bachmann, J. Ravantti, L. Pelkmans, C. Fraefel, Cellular state landscape and herpes simplex virus type 1 infection progression are connected, Nat. Commun. 14 (2023) 4515, https://doi.org/10.1038/s41467-023-40148-6.
- [48] J.P. Fredrikson, L.F. Domanico, S.L. Pratt, E.K. Loveday, M.P. Taylor, C.B. Chang, Single-cell herpes simplex virus type 1 infection of neurons using drop-based microfluidics reveals heterogeneous replication kinetics, Sci. Adv. 10 (2024) eadk9185, https://doi.org/10.1126/sciadv.adk9185.
- [49] S. Galli, G. Flint, L. Růžičková, M.D. Antonio, Genome-wide mapping of G-quadruplex DNA: a step-by-step guide to select the most effective method, RSC Chem. Biol. 5 (2024) 426–438, https://doi.org/10.1039/D4CB00023D.
- [50] K. Yazdani, S. Seshadri, D. Tillo, M. Yang, C.D. Sibley, C. Vinson, J. S. Schneekloth Jr., Decoding complexity in biomolecular recognition of DNA imotifs with microarrays, Nucleic Acids Res. 51 (2023) 12020–12030, https://doi.org/10.1093/nar/gkad981.
- [51] J. Moffat, C.-C. Ku, L. Zerboni, M. Sommer, A. Arvin, VZV: pathogenesis and the disease consequences of primary infection, in: A. Arvin, G. Campadelli-Fiume, E. Mocarski, P.S. Moore, B. Roizman, R. Whitley, K. Yamanishi (Eds.), Hum. Herpesviruses Biol. Ther. Immunoprophyl., Cambridge University Press, Cambridge, 2007 http://www.ncbi.nlm.nih.gov/books/NBK47382/ (accessed March 28, 2025).
- [52] G. Torma, D. Tombácz, Z. Csabai, I.A.A. Almsarrhad, G.Á. Nagy, B. Kakuk, G. Gulyás, L.M. Spires, I. Gupta, Á. Fülöp, Á. Dörmő, I. Prazsák, M. Mizik, V.É. Dani, V. Csányi, Á. Harangozó, Z. Zádori, Z. Toth, Z. Boldogkői, Identification of herpesvirus transcripts from genomic regions around the replication origins, Sci. Rep. 13 (2023) 16395, https://doi.org/10.1038/s41598-023-43344-v.
- [53] M.C. Rodríguez, J.M. Dybas, J. Hughes, M.D. Weitzman, C. Boutell, The HSV-1 ubiquitin ligase ICP0: modifying the cellular proteome to promote infection, Virus Res. 285 (2020) 198015, https://doi.org/10.1016/j.virusres.2020.198015.
- [54] R.M. Sandri-Goldin, The many roles of the regulatory protein ICP27 during herpes simplex virus infection, Front. Biosci. J. Virtual Libr. 13 (2008) 5241–5256, https://doi.org/10.2741/3078.
- [55] A.J. Rutkowski, F. Erhard, A. L'Hernault, T. Bonfert, M. Schilhabel, C. Crump, P. Rosenstiel, S. Efstathiou, R. Zimmer, C.C. Friedel, L. Dölken, Widespread disruption of host transcription termination in HSV-1 infection, Nat. Commun. 6 (2015) 7126. https://doi.org/10.1038/ncomms8126.
- [56] M.I. Khalil, M.H. Sommer, J. Hay, W.T. Ruyechan, A.M. Arvin, Varicella-zoster virus (VZV) origin of DNA replication oriS influences origin-dependent DNA replication and flanking gene transcription, Virology 481 (2015) 179–186, https:// doi.org/10.1016/j.virol.2015.02.049.
- [57] A. Bedrat, L. Lacroix, J.-L. Mergny, Re-evaluation of G-quadruplex propensity with G4Hunter, Nucleic Acids Res. 44 (2016) 1746–1759, https://doi.org/10.1093/nar/gkw006.

- [58] S.A. Ross, C.J. Burrows, Cytosine-specific chemical probing of DNA using bromide and monoperoxysulfate, Nucleic Acids Res. 24 (1996) 5062–5063, https://doi.org/ 10.1093/nar/24.24.5062.
- [59] H. Abou Assi, M. Garavís, C. González, M.J. Damha, I-motif DNA: structural features and significance to cell biology, Nucleic Acids Res. 46 (2018) 8038–8056, https://doi.org/10.1093/nar/gky735.
- [60] P. Školáková, D. Renčiuk, J. Palacký, D. Krafčík, Z. Dvořáková, I. Kejnovská, K. Bednářová, M. Vorlíčková, Systematic investigation of sequence requirements for DNA i-motif formation, Nucleic Acids Res. 47 (2019) 2177–2189, https://doi. org/10.1093/nar/gkz046.
- [61] S.P. Gurung, C. Schwarz, J.P. Hall, C.J. Cardin, J.A. Brazier, The importance of loop length on the stability of i-motif structures, Chem. Commun. 51 (2015) 5630–5632, https://doi.org/10.1039/C4CC07279K.
- [62] K.L. Irving, J.J. King, Z.A.E. Waller, C.W. Evans, N.M. Smith, Stability and context of intercalated motifs (i-motifs) for biological applications, Biochimie 198 (2022) 33–47, https://doi.org/10.1016/j.biochi.2022.03.001.
- [63] T. Fujii, N. Sugimoto, Loop nucleotides impact the stability of intrastrand i-motif structures at neutral pH, Phys. Chem. Chem. Phys. 17 (2015) 16719–16722, https://doi.org/10.1039/C5CP02794B.
- [64] J. Rodriguez, A. Domínguez, A. Aviñó, G. Borgonovo, R. Eritja, S. Mazzini, R. Gargallo, Exploring the stabilizing effect on the i-motif of neighboring structural motifs and drugs, Int. J. Biol. Macromol. 242 (2023) 124794, https://doi.org/ 10.1016/j.ijbiomac.2023.124794.
- [65] S.P. Gurung, C. Schwarz, J.P. Hall, C.J. Cardin, J.A. Brazier, The importance of loop length on the stability of i-motif structures, Chem. Commun. Camb. Engl. 51 (2015) 5630–5632, https://doi.org/10.1039/c4cc07279k.
- [66] S. Tang, M. Bosch-Marce, A. Patel, T.P. Margolis, P.R. Krause, Characterization of herpes simplex virus 2 primary microRNA transcript regulation, J. Virol. 89 (2015) 4837–4848, https://doi.org/10.1128/JVI.03135-14.
- [67] S. Takahashi, S. Ghosh, M. Trajkovski, T. Ohyama, J. Plavec, N. Sugimoto, Twisting tetraplex DNA: a strand dynamics regulating i-motif function in diverse molecular crowding environments, Nucleic Acids Res. 53 (2025) gkaf500, https://doi.org/ 10.1093/nar/gkaf500.
- [68] P. Wolski, K. Nieszporek, T. Panczyk, G-Quadruplex and I-motif structures within the Telomeric DNA duplex. A molecular dynamics analysis of protonation states as factors affecting their stability, J. Phys. Chem. B 123 (2019) 468–479, https://doi. org/10.1021/acs.ipcb.8b11547.
- [69] S. Chaturvedi, R. Engel, L. Weinberger, The HSV-1 ICP4 transcriptional autorepression circuit functions as a transcriptional "accelerator" circuit, Front. Cell. Infect. Microbiol. 10 (2020), https://doi.org/10.3389/fcimb.2020.00265.
- [70] R.B. Tunnicliffe, M.P. Lockhart-Cairns, C. Levy, A.P. Mould, T.A. Jowitt, H. Sito, C. Baldock, R.M. Sandri-Goldin, A.P. Golovanov, The herpes viral transcription factor ICP4 forms a novel DNA recognition complex, Nucleic Acids Res. 45 (2017) 8064–8078. https://doi.org/10.1093/nar/gkx419.
- [71] K.L. Irving, J.J. King, Z.A.E. Waller, C.W. Evans, N.M. Smith, Stability and context of intercalated motifs (i-motifs) for biological applications, Biochimie 198 (2022) 33–47, https://doi.org/10.1016/j.biochi.2022.03.001.